

Fulde–Ferrell–Larkin–Ovchinnikov State in Perpendicular Magnetic Fields in Strongly Pauli-Limited Quasi-Two-Dimensional Superconductors

Hiroshi Shimahara

*Graduate School of Advanced Science and Engineering, Hiroshima University,
Higashi-Hiroshima 739-8530, Japan*

(Received November 5, 2020)

We examine the Fermi-surface effect called the nesting effect for the Fulde–Ferrell–Larkin–Ovchinnikov (FFLO) state in strongly Pauli-limited quasi-two-dimensional superconductors, focusing on the effect of three-dimensional factors, such as interlayer electron transfer, interlayer pairing, and off-plane magnetic fields including those perpendicular to the most conductive layers (hereinafter called the perpendicular fields). We examine the systems with a large Maki parameter so that the orbital pair-breaking effect is negligible, except for the locking of the direction of the FFLO vector \mathbf{q} in the magnetic-field direction. It is known that the nesting effect for the FFLO state can be strong in quasi-low-dimensional systems in which the orbital pair-breaking effect is suppressed by applying the magnetic field parallel to the layers. Hence, it has sometimes been suggested that the nesting effect may hardly enhance the stability of the FFLO state for perpendicular fields. We illustrate that, contrary to this view, the nesting effect can strongly stabilize the FFLO state for perpendicular fields as well as for parallel fields when t_z is small so that the Fermi surfaces are open in the k_z -direction, where t_z denotes the interlayer transfer energy. In particular, the nesting effect in perpendicular fields can be strong in interlayer states. For example, in systems with cylindrical Fermi surfaces warped by $t_z \neq 0$, interlayer states with $\Delta_k \propto \sin k_z$ exhibit $\mu_e H_c \approx 1.65\Delta_{a0}$ for perpendicular fields, which is much larger than typical values for parallel fields, such as $\mu_e H_c = \Delta_{s0}$ of the s-wave state and $\mu_e H_c \approx 1.28\Delta_{d0}$ of the d-wave state in cylindrical systems with $t_z = 0$. Here, μ_e and H_c are the electron magnetic moment and upper critical field of the FFLO state at $T = 0$, respectively, and $\Delta_{a0} \equiv 2\omega_c e^{-1/\lambda_a}$. We discuss the possible relevance of the nesting effect to the high-field superconducting phases in perpendicular fields observed in the compounds CeCoIn₅ and FeSe, which are candidates for the FFLO state. The present result could potentially provide a physical reason for the fact that the areas in the phase diagrams occupied by the high-field phases for the perpendicular and parallel fields are of the same order.

1. Introduction

The Fulde–Ferrell–Larkin–Ovchinnikov (FFLO) state^{1,2)} has been examined in quasi-two-dimensional systems for candidate compounds, such as some organic and heavy fermion superconductors.^{3–11)} In many cases in theoretical studies, two-dimensional models¹²⁾ are useful as effective models of quasi-two-dimensional systems; however, depending on the problem under examination, the three-dimensionality of the systems due to interlayer electron transfer must be treated explicitly, for example, when interlayer pairing and/or off-plane magnetic fields play essential roles.

Since the FFLO state is a superconducting state induced by Cooper pairs with a finite center-of-mass momentum \mathbf{q} ¹³⁾ (hereinafter called the FFLO vector), it significantly depends on the Fermi-surface structure, for example, because of the direction of \mathbf{q} relative to the anisotropic Fermi surface. At the same time, unless the orbital pair-breaking effect is too weak or too strong,^{14–16)} the direction of \mathbf{q} is locked in the direction of the magnetic field \mathbf{H} ; i.e., $\mathbf{q} \parallel \mathbf{H}$.^{14,17)} From this point of view, it is physically interesting that all the candidates discovered thus far are quasi-low-dimensional, which can be attributed to the following two reasons: (i) the suppression of the orbital pair-breaking effect when \mathbf{H} is parallel to the most conductive layers^{5,18)} (hereinafter called the ab-plane) and (ii) the Fermi-surface nesting effect for the FFLO state.^{19–21)}

For two of the strongest candidate compounds, CeCoIn₅ and FeSe, reason (i) would not apply, because the conduction electrons have large effective masses,^{8,9,22–24)} which result in large Maki parameters; hence, \mathbf{H} would not need to be parallel to the ab-plane for the emergence of the FFLO state. In

fact, high-field superconducting phases, which can be considered to be the FFLO state, were observed^{22,25)} in these compounds when $\mathbf{H} \parallel \mathbf{c}$ as well as when $\mathbf{H} \perp \mathbf{c}$, where \mathbf{a} , \mathbf{b} , and \mathbf{c} denote the lattice vectors in the directions of the crystal a-, b-, and c-axes.

The Fermi-surface nesting effect for the FFLO state mentioned in reason (ii) is an effect analogous with the nesting effect for spin- and charge-density waves (SDW and CDW). In quasi-low-dimensional systems, when nesting instabilities such as SDW and CDW instabilities are suppressed by sufficient distortion of the Fermi surfaces,²¹⁾ the highly anisotropic Fermi-surface structures help stabilize the FFLO state. The nesting effect for the FFLO state can be examined by considering the overlap of one of the Fermi surfaces of the up- and down-spin electrons and another that is shifted by \mathbf{q} .^{20,21)} In a simple two-dimensional model in which the interlayer electron transfer is neglected, the Fermi surfaces can touch on a vertical line for $\mathbf{H} \perp \mathbf{c}$ because $\mathbf{q} \parallel \mathbf{H}$ as mentioned above, whereas for $\mathbf{H} \parallel \mathbf{c}$, they cannot touch each other. Hence, it may be thought that the nesting effect does not work when $\mathbf{H} \parallel \mathbf{c}$ in quasi-two-dimensional systems. For example, in CeCoIn₅ and FeSe, the high-field phases for $\mathbf{H} \parallel \mathbf{c}$ may appear to be inconsistent with reason (ii) as well as with reason (i). However, as shown in the following, the nesting effect can work even when $\mathbf{H} \parallel \mathbf{c}$, in the presence of the warp of the Fermi surfaces in the direction of \mathbf{c} .

Motivated by these experimental and theoretical studies, we examine the effects of three-dimensional factors, such as interlayer electron transfer, interlayer pairing, and off-plane magnetic fields including perpendicular fields. Off-

plane magnetic fields can cause extreme phenomena, such as vortex states with higher Landau-level indices, through the orbital pair-breaking effect.^{15, 18, 26, 27)} However, because the orbital effect has been examined in previous studies, in the present study we focus on the nesting effect in the absence of the orbital effect. We also incorporate the possibility of interlayer pairing because, owing to the finite \mathbf{q} , strong interplay between the three-dimensional structures of the gap function and the Fermi surface is expected. In addition, the FFLO state is worth studying for interlayer pairing because of the compound Sr_2RuO_4 , for which both the FFLO state²⁸⁾ and interlayer pairing^{29, 30)} can be considered.

For quasi-two-dimensional systems in perpendicular fields, Song and Koshelev proposed a theory of interplay between orbital-quantization effects and the FFLO state, and discussed the FFLO state in FeSe when $\mathbf{H} \parallel \mathbf{c}$.³¹⁾ In the present study, we assume weaker magnetic fields.

In Sect. 2, we briefly review formulas and define the systems and states to be examined. In Sect. 3, we examine systems with Fermi surfaces straight in the k_z -direction. In Sect. 4, we examine systems with warped Fermi surfaces. We discuss the possible relevance of our results to the high-field phases in the compounds CeCoIn_5 and FeSe. The final section summarizes and concludes the paper. We define the x -, y -, and z -axes along the crystal a -, b -, and c -axes. The lattice constants a , b , and c are absorbed into the definitions of the momentum components k_x , k_y , and k_z . We use units in which $\hbar = k_B = 1$, and we denote the electron magnetic moment by $\mu_e = g\mu_B/2$. For convenience, we define the functions

$$f_n(p) = - \int_0^\pi \frac{dx}{\pi} \cos(nx) \ln|1 - p \cos x|. \quad (1)$$

Their explicit forms are shown in Appendix A.

2. Formulas and Model

Formula for the Critical Field — We use the formula³²⁾ for the upper critical field at $T = 0$

$$h_c \equiv \mu_e H_c = \frac{1}{2} \Delta_{\alpha 0} \max_{\mathbf{q}} [e^{f_\alpha(\mathbf{q})}] \quad (2)$$

with

$$f_\alpha(\mathbf{q}) = - \frac{1}{\langle |\gamma_\alpha(\hat{\mathbf{k}})|^2 \rangle} \left\langle |\gamma_\alpha(\hat{\mathbf{k}})|^2 \ln \left[1 - \frac{\mathbf{v}_F \cdot \mathbf{q}}{2h_c} \right] \right\rangle \quad (3)$$

for the α -wave state with the gap function $\Delta_{\mathbf{k}} = \Delta_\alpha \gamma_\alpha(\hat{\mathbf{k}})$, where γ_α denotes a basis function of $\hat{\mathbf{k}} \equiv \mathbf{k}/|\mathbf{k}|$, and $\Delta_{\alpha 0} \equiv 2\omega_c e^{-1/\lambda_\alpha}$ is a scale of the gap function.³³⁾ The average is defined as

$$\langle g(\hat{\mathbf{k}}) \rangle = \int \frac{d^2 \hat{\mathbf{k}}}{S_0} \frac{\rho(0, \hat{\mathbf{k}})}{N(0)} g(\hat{\mathbf{k}}) \quad (4)$$

for an arbitrary $g(\hat{\mathbf{k}})$, where $\rho(\xi, \hat{\mathbf{k}})$ is the angle-dependent density of states, $N(\xi)$ is the density of states, and S_0 is an appropriate normalization constant.³⁴⁾ The FFLO vector is the vector \mathbf{q} that gives the highest h_c in accordance with the variational principle;²¹⁾ however, only the magnitude $q \equiv |\mathbf{q}|$ is optimized in Eq. (2) because $\mathbf{q} \parallel \mathbf{H}$ in the present problem. The formula in Eq. (2) is derived in the weak coupling theory,^{32, 35)} where a second-order transition is assumed. If the second-order transition at h_c is to occur, h_c must exceed the Pauli limit $h_P = \mu_e H_P$.³⁶⁾

The Pauli paramagnetic limit h_P in anisotropic superconductors is given by the formula^{32, 35)}

$$h_P = \frac{\sqrt{\langle |\gamma_\alpha|^2 \rangle} \Delta_{\alpha 0}}{\bar{\gamma}_\alpha \sqrt{2}},$$

where $\bar{\gamma}_\alpha = \exp[\langle |\gamma_\alpha|^2 \ln |\gamma_\alpha| \rangle / \langle |\gamma_\alpha|^2 \rangle]$. The inequality

$$h_P \leq \frac{\Delta_{\alpha 0}}{\sqrt{2}} \quad (5)$$

can be proved in general as shown in Appendix B. The equality sign holds if and only if $\gamma_\alpha(\hat{\mathbf{k}})$ is constant.

The real upper critical field would be smaller than the value of h_c given by Eq. (2) owing to negative effects, such as the orbital pair-breaking effect and the fluctuation effect. However, the value of h_c is useful because a higher h_c must imply that the free energy of the FFLO state at $h \equiv \mu_e H \sim \Delta_0$ is lower. The value of h_c can be regarded as an index of the strength of the positive effects that stabilize the FFLO state.

Systems and States to be Examined — In the following, we consider a three-dimensional structure of the order parameter by assuming

$$\gamma_\alpha(\hat{\mathbf{k}}) = \gamma_\alpha(\varphi, k_z) = \gamma_{\alpha_\parallel}^\parallel(\varphi) \gamma_{\alpha_z}^z(k_z)$$

with $\alpha = (\alpha_\parallel, \alpha_z)$, where $\gamma_{\alpha_\parallel}^\parallel$ and $\gamma_{\alpha_z}^z$ are basis functions that satisfy

$$\int_0^{2\pi} \frac{d\varphi}{2\pi} |\gamma_{\alpha_\parallel}^\parallel(\varphi)|^2 = \int_0^{2\pi} \frac{dk_z}{2\pi} |\gamma_{\alpha_z}^z(k_z)|^2 = 1.$$

The Fourier transformation of $\langle c_{i\uparrow} c_{j\downarrow} \rangle$ verifies that $\gamma_{\alpha_z}^z(k_z)$ does not depend on k_z if $\langle c_{i\uparrow} c_{j\downarrow} \rangle \neq 0$ only for sites i and j on the same layer, whereas $\gamma_{\alpha_z}^z(k_z)$ depends on k_z owing to the factor $e^{\pm i\mathbf{k} \cdot (\mathbf{R}_i - \mathbf{R}_j)}$ if $\langle c_{i\uparrow} c_{j\downarrow} \rangle \neq 0$ for sites i and j on different layers, where $c_{i\sigma}$ denotes the operator of the electron with spin σ on site i at \mathbf{R}_i . We call the states of the former and latter cases the intralayer and interlayer states, which are induced by intralayer and interlayer attractive interactions, respectively.³⁷⁾ We define the one-particle (electron or hole) energy

$$\xi_{\mathbf{k}} = \epsilon_{\mathbf{k}_\parallel}^\parallel - 2t_z \cos k_z - \mu, \quad (6)$$

where

$$\epsilon_{\mathbf{k}_\parallel}^\parallel = \frac{k_x^2}{2m_x} + \frac{k_y^2}{2m_y} \quad (7)$$

with $\mathbf{k}_\parallel = (k_x, k_y)$.³⁸⁾ Equation (7) can be transformed into an isotropic dispersion $\epsilon_{\mathbf{k}_\parallel}^\parallel = \tilde{k}_\parallel^2/2m$ by defining $\tilde{\mathbf{k}}_\parallel = (\tilde{k}_x, \tilde{k}_y)$, $\tilde{k}_\mu = \sqrt{m/m_\mu} k_\mu$, and $m = \sqrt{m_x m_y}$, and hence, all the equations for $m_x \neq m_y$ can be transformed into the corresponding equations for $m_x = m_y = m$ (Appendix C). Therefore, we use

$$\epsilon_{\mathbf{k}_\parallel}^\parallel = \frac{k_\parallel^2}{2m} \quad (8)$$

in the following for conciseness.

The present model can be effective for systems in which the electron (or hole) density is small. For an arbitrary $\epsilon_{\mathbf{k}_\parallel}^\parallel$, redefining the momentum coordinate appropriately and, if necessary, making the electron-hole transformation, we can assume that the minimum of $\epsilon_{\mathbf{k}_\parallel}^\parallel$ is at $\mathbf{k}_\parallel = (0, 0)$. Expanding $\epsilon_{\mathbf{k}_\parallel}^\parallel$ around $\mathbf{k}_\parallel = (0, 0)$ and redefining the k_x - and k_y -axes along

the principal axes, we obtain Eq. (7) as an approximate form when the carrier density is small.³⁹⁾

3. Systems with Straight Fermi Surfaces

Before examining systems with $t_z \neq 0$, let us examine systems with $t_z = 0$. When $t_z = 0$, the Fermi surfaces are straight (elliptic) cylinders. The cylindrical system has been examined in previous studies when the magnetic field is parallel to the layers; however, the study in this section covers wider situations, including an arbitrary direction of \mathbf{H} except for the c -direction, interlayer pairing as well as intralayer pairing, and systems with effective mass anisotropy $m_x \neq m_y$. Equation (3) reduces to

$$f_\alpha(\mathbf{q}) = - \int_0^{2\pi} \frac{d\varphi}{2\pi} |\gamma_{\alpha_{\parallel}}^{\parallel}(\varphi)|^2 \ln|1 - \bar{q} \cos \varphi|, \quad (9)$$

where $\bar{q} = v_F q_{\parallel} / 2h_c$, $v_F = k_F^{\parallel} / m$, $q_{\parallel} = |\mathbf{q}_{\parallel}|$, and $\mathbf{q}_{\parallel} = (q_x, q_y)$. Here, $\gamma_{\alpha_z}^z(k_z)$ has disappeared from the equation; hence, the argument in this section does not depend on α_z .

First, we examine the states in which the symmetry of $\Delta_{\mathbf{k}}$ is s-wave in each layer and arbitrary in the k_z -direction.⁴⁰⁾ In such states, $\gamma_s^{\parallel}(\varphi) = 1$, and hence, $f_\alpha(\mathbf{q}) = f_0(\bar{q})$; i.e.,

$$f_\alpha(\mathbf{q}) = - \int_0^{2\pi} \frac{d\theta}{2\pi} \ln|1 - \bar{q} \cos \theta|. \quad (10)$$

Therefore, we obtain

$$f_\alpha(\bar{q}) = \begin{cases} -\ln(\bar{q}/2) & \text{for } \bar{q} \geq 1, \\ -\ln\{[1 + (1 - \bar{q}^2)^{1/2}]/2\} & \text{for } \bar{q} \leq 1, \end{cases} \quad (11)$$

which is the same as the equation in the previous paper²¹⁾ except for the definition of \bar{q} and the extended applicability mentioned above. From Eq. (2), it follows that $h_c = \Delta_{\alpha 0}$ and $\bar{q} = 1$. This result holds for an arbitrary symmetry in the k_z -direction and an arbitrary magnetic-field direction except for $\mathbf{H} \parallel \mathbf{c}$.⁴¹⁾

The fact that $H_c = \Delta_{\alpha 0} / \mu_e$ is much larger than the Pauli limit $H_P \leq \Delta_{\alpha 0} / \sqrt{2} \mu_e$ can be attributed to the nesting effect.^{21,32,35,42-44)} As shown in Fig. 1, the Fermi surfaces touch on a line (hereinafter called the nesting line) by a displacing vector \mathbf{q}_0 that has $q_{\parallel} = 2h_c / v_F$. The FFLO vector \mathbf{q} obtained above also has the same q_{\parallel} ($= 2h_c / v_F$), and the large value of h_c can be attributed to the fact that the Fermi surfaces touch each other.

Next, we examine the states in which the symmetry of $\Delta_{\mathbf{k}}$ is d-wave in each layer and arbitrary in the k_z -direction.⁴⁰⁾ For such states, we adopt $\gamma_d^{\parallel}(\varphi) = \sqrt{2} \cos(2\varphi)$ as the principal in-plane basis function. As many authors have reported,⁴⁵⁾ h_c depends on the direction of \mathbf{H}_{\parallel} , where $\mathbf{H} = (\mathbf{H}_{\parallel}, H_z)$. Let \mathbf{q}_0 denote the nesting vector that is parallel to \mathbf{H} and has $q_{\parallel} = 2h_c / v_F$. When $\mathbf{H}_{\parallel} \parallel \mathbf{a}$, because $\Delta_{\mathbf{k}}$ is maximum on the nesting line, the FFLO vector \mathbf{q} is equal to \mathbf{q}_0 , as in the s-wave state. By contrast, when $\mathbf{H}_{\parallel} \parallel [1, 1, 0]$, because $\Delta_{\mathbf{k}}$ vanishes on the nesting line, we obtain $\mathbf{q} \neq \mathbf{q}_0$. This is shown by an explicit calculation as outlined below. It can be easily verified that

$$f_\alpha(\mathbf{q}) = \begin{cases} f_0(\bar{q}) + f_4(\bar{q}) & \text{for } \mathbf{H}_{\parallel} \parallel \mathbf{a}, \\ f_0(\bar{q}) - f_4(\bar{q}) & \text{for } \mathbf{H}_{\parallel} \parallel [1, 1, 0], \end{cases} \quad (12)$$

and the functions f_0 and f_4 can be obtained as shown in Appendix A. This results in h_c and \bar{q} as summarized in Table I. The value $\bar{q} = 1$ for $\mathbf{H}_{\parallel} \parallel \mathbf{a}$ implies that the Fermi surfaces touch on a line. By contrast, the value $\bar{q} \approx 1.210 > 1$ for

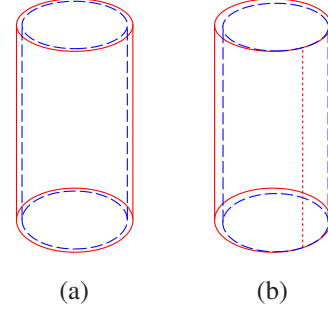


Fig. 1. (Color online) Schematics of cylindrical Fermi surfaces for $t_z = 0$ in the first Brillouin zone. (a) The red solid and blue dashed curves show the Fermi surfaces of the down- and up-spin electrons, respectively, that split because of the Zeeman energy. (b) The Fermi surface of the up-spin electrons is shifted by a nesting vector \mathbf{q}_0 that has $q_{\parallel} = 2h_c / v_F$, for which the Fermi surfaces touch on the vertical line shown by the red dotted line.

$\mathbf{H}_{\parallel} \parallel [1, 1, 0]$ implies that the Fermi surfaces are intersected by two vertical lines. Because of the nesting effect for the FFLO state, h_c for $\mathbf{H}_{\parallel} \parallel \mathbf{a}$ is approximately 30% larger than that for $\mathbf{H}_{\parallel} \parallel [1, 1, 0]$.

Table I. Results for the states with a symmetry that is d-wave in each layer and arbitrary in the k_z -direction, when $t_z = 0$ and $\mathbf{H} \nparallel \mathbf{c}$.

	$\mathbf{H}_{\parallel} \parallel \mathbf{a}$	$\mathbf{H}_{\parallel} \parallel [1, 1, 0]$
Max. of f_d	$\ln 2 + \frac{1}{4}$	$\frac{1}{2} \ln(\sqrt{3} + 1) + \frac{\sqrt{3} - 1}{4}$
\bar{q}	1	$\sqrt{2}(\sqrt{3} - 1)^{1/2} \approx 1.210$
Fermi surfaces	Touch on a line	Intersected by two lines
$\frac{h_c}{\Delta_{d0}}$	$e^{1/4} \approx 1.284$	$\frac{1}{2}(\sqrt{3} + 1)^{1/2} e^{\frac{\sqrt{3}-1}{4}} \approx 0.992$

4. Systems with Warped Fermi Surfaces

In this section, we examine systems with $t_z \neq 0$ in perpendicular fields, i.e., $\mathbf{H} \parallel \mathbf{c}$, for which $\mathbf{q} = (0, 0, q)$. We assume that t_z is sufficiently small so that the Fermi surfaces are open in the k_z -direction. For the states with $\alpha = (\alpha_{\parallel}, \alpha_z)$, we obtain

$$f_\alpha(\mathbf{q}) = - \int_0^{2\pi} \frac{dk_z}{2\pi} |\gamma_{\alpha_z}^z(k_z)|^2 \ln|1 - \bar{q} \sin k_z|, \quad (13)$$

where \bar{q} is redefined as $\bar{q} = t_z q / h_c$. Because $\gamma_{\alpha_{\parallel}}^{\parallel}(\varphi)$ has disappeared from the equation, the following argument does not depend on the in-plane symmetry α_{\parallel} .

For the intralayer states, because $\gamma_{\alpha_z}^z(k_z) = 1$, Eq. (13) is reduced to $f_\alpha(\mathbf{q}) = f_0(\bar{q})$, i.e.,

$$f_\alpha(\mathbf{q}) = - \int_0^{2\pi} \frac{dk_z}{2\pi} \ln|1 - \bar{q} \sin k_z|, \quad (14)$$

which is mathematically equivalent to Eq. (10); however, $\cos \theta$ in Eq. (10) originates from the relative angle θ between \mathbf{q}_{\parallel} and \mathbf{k}_{\parallel} , whereas $\sin k_z$ in Eq. (14) originates from the variation of the Fermi velocity in the k_z -direction. The same calculation leads to exactly the same equation as Eq. (11) except for the definition of \bar{q} , and hence, we obtain $h_c = \Delta_{\alpha 0}$ and

$\bar{q} = 1$. Interestingly, the results coincide for the completely different systems, as summarized in Table II. The fact that h_c exceeds the Pauli limit $h_p = \Delta_{\alpha 0} / \sqrt{2}$ implies that the FFLO state can be stabilized, which is expected from the results of previous studies.⁴⁶⁾ A new finding of the present study is that h_c *substantially* exceeds h_p and it is of the same order as that for parallel fields. This implies that the nesting effect significantly enhances the stability of the FFLO state, for perpendicular as well as parallel fields.

Table II. Comparison of the results for the two types of nesting effect for $\mathbf{H} \nparallel \mathbf{c}$ and $\mathbf{H} \parallel \mathbf{c}$.

Assumptions		
Interlayer transfer	$t_z = 0$	$t_z \neq 0$
Fermi surfaces	Cylinders	Warped cylinders
Direction of \mathbf{H}	Arbitrary ($\nparallel \mathbf{c}$)	$\mathbf{H} \parallel \mathbf{c}$
$\gamma_{\alpha_{\parallel}}^{\parallel}$	Constant (s-wave)	Arbitrary
$\gamma_{\alpha_z}^z$	Arbitrary	Constant (intralayer pairing)
Results		
Equation	Eq. (10)	Eq. (14)
Optimum \bar{q}	1 ($q_{\parallel} = 2h_c/v_F$)	1 ($q = q_z = h_c/t_z$)
Nesting	Vertical line	Horizontal circle
h_c	$\Delta_{\alpha 0}$	$\Delta_{\alpha 0}$

Although the *exact* coincidence in h_c is only a consequence of the simplifications of the models, which lead to the mathematical similarity of Eqs. (10) and (14), it is physically significant that h_c is of the same order in the two cases. The physical reason is interpreted using Fig. 2. The split Fermi surfaces shown in Fig. 2(a) touch on a circle (the red dotted curve, hereinafter called the nesting curve) when one of the Fermi surfaces is shifted by $\mathbf{q} \parallel \mathbf{c}$ as shown in Fig. 2(b). The nesting curve is a full circle (or ellipse) because all the cross sections are circular (or elliptic). In general, when the shapes of the cross sections perpendicular to the k_z -axis are the same, the Fermi surfaces touch in a similar manner when one of them is shifted by the nesting vector \mathbf{q}_0 ($\parallel \mathbf{c}$) appropriate for the Fermi-surface geometry. For this mechanism, the nesting curve is not necessarily closed like a full circle. When parts of the cross sections are similar, the nesting effect can work.

The quasi-low-dimensionality plays an essential role in the present nesting effect even for perpendicular fields. In Fig. 2(b), the smaller Fermi surface is completely inside the larger Fermi surface. This implies that on the nesting curve, the Fermi surfaces touch but do not cross. The open structure of the Fermi surfaces in the k_z -direction favors this behavior because of the presence of the inflection points at $k_z = \pm\pi/2$. In contrast, when t_z is large, the Fermi surfaces are closed and round near the k_z -axis, and analogously with the spherical system, h_c is lower than $\Delta_{\alpha 0}$.⁴⁷⁾ Hence, for the present mechanism of the nesting effect in perpendicular fields, t_z must be sufficiently small. The upper limit of t_z below which the Fermi surfaces are open and touch on a curve decreases as the carrier density decreases.

Interlayer pairing — In this part, we consider the interlayer states. For the interlayer pairing between electrons on

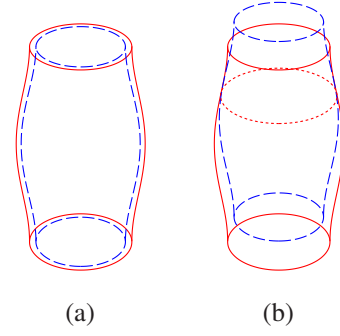


Fig. 2. (Color online) Similar to Fig. 1, but the Fermi surfaces are warped and $\mathbf{q} \parallel \mathbf{c}$. In (b), the Fermi surface of up-spin electrons is shifted by \mathbf{q}_0 with $|\mathbf{q}_0| = h_c/t_z$. For this value of $|\mathbf{q}_0|$, the Fermi surfaces touch on the circle shown by the red dotted curve.

adjacent layers, $\Delta_{\mathbf{k}}$ is proportional to $\gamma_{cz}^z = \sqrt{2} \cos k_z$ or $\gamma_{sz}^z = \sqrt{2} \sin k_z$, where the indices $\alpha_z = cz$ and sz are defined. When $t_z \neq 0$ and $\mathbf{H} \parallel \mathbf{c}$, because the nesting curve is at $k_z = \pi/2$ as shown in Fig. 2(b), the nesting effect does not work for the states with $\Delta_{\mathbf{k}} \propto \cos k_z$, whereas it significantly enhances h_c for the states with $\Delta_{\mathbf{k}} \propto \sin k_z$. This behavior is shown in the following.

For the interlayer states, we obtain

$$f_{\alpha}(\mathbf{q}) = \begin{cases} f_0(\bar{q}) + f_2(\bar{q}) & \text{for } \alpha_z = sz \\ f_0(\bar{q}) - f_2(\bar{q}) & \text{for } \alpha_z = cz, \end{cases} \quad (15)$$

where the functions f_0 and f_2 are given in Appendix A. The results for h_c and \bar{q} are summarized in Table III. Equation (15) and Table III are quite similar to Eq. (12) and Table I for the d-wave state in parallel fields. The argument that applies the relation between the value of \bar{q} and the nesting for the d-wave state also applies to that for the present interlayer states. As shown in Table III, the upper critical field $h_c = e^{1/2} \Delta_{\alpha 0}$ for the sz-wave states is much larger than $h_c = \Delta_{\alpha 0} / \sqrt{2}$ for the cz-wave states, although both values are larger than h_p because of Eq. (5). Their ratio, $e^{1/2}/(1/\sqrt{2}) \approx 2.33$, is much larger than the corresponding ratio of h_c ($1.284/0.992 \approx 1.29$) for the d-wave state in parallel fields shown in Table I.

To quantitatively estimate the critical fields of the interlayer states, the orbital pair-breaking effect must be incorporated. The possible difference in the orbital pair-breaking effect between the intralayer and interlayer states can be an interesting subject to study.

Table III. Results for interlayer states with an arbitrary in-plane symmetry α_{\parallel} when $t_z \neq 0$ and $\mathbf{H} \parallel \mathbf{c}$.

α_z	sz	cz
Nodes	$k_z = 0, \pm\pi$	$k_z = \pm\pi/2$
Max. of f_{α}	$\ln 2 + \frac{1}{2}$	$\frac{1}{2} \ln 2$
\bar{q}	1	$\sqrt{2} \approx 1.414$
Fermi surfaces	Touch on a circle	Intersected by two circles
$\frac{h_c}{\Delta_{\alpha 0}}$	$e^{1/2} \approx 1.649$	$\frac{1}{\sqrt{2}} \approx 0.707$

Compounds CeCoIn₅ and FeSe — The present mechanism may explain the existence of the high-field superconducting phases for $\mathbf{H} \parallel \mathbf{c}$ in the compounds CeCoIn₅ and FeSe, which are considered to be the FFLO state. At least, as illustrated above, the perpendicular direction ($\mathbf{H} \parallel \mathbf{c}$) is not necessarily disadvantageous to the nesting effect for the FFLO state in quasi-low-dimensional systems. For FeSe, a small carrier density and nearly cylindrical Fermi surfaces^{22–24}) are compatible with the present model in Eqs. (6) or (7). For this compound, the specific feature $\Delta \sim \epsilon_F^{22,24}$) should be incorporated in future research. In CeCoIn₅, a first-principles calculation⁴⁸) suggests that some of the Fermi surfaces are cylindrical but corrugated. The present theory may be applicable to those Fermi surfaces. For accurate prediction of the FFLO state, extremely accurate information on the Fermi-surface structure would be required,^{32,44}) and analysis incorporating realistic shapes of Fermi surfaces is a future research direction.

5. Summary and Conclusion

We examined the FFLO state in strongly Pauli-limited quasi-two-dimensional superconductors in magnetic fields perpendicular to the ab-plane, focusing on the Fermi-surface nesting effect for the FFLO state; the orbital pair-breaking effect is neglected, except for the locking of the direction of \mathbf{q} in the direction of \mathbf{H} . The nesting effect for the FFLO state can enhance h_c for perpendicular fields in systems with cylindrical Fermi surfaces warped by $t_z \neq 0$. For intralayer states, the nesting effect in perpendicular fields is as strong as that for the s-wave state in parallel fields (Table II). For the interlayer states, the nesting effect in perpendicular fields can be more pronounced because of the k_z -dependence in Δ_k . In fact, it was shown that states with $\Delta_k \propto \sin k_z$ exhibit $h_c/\Delta_{\alpha 0} \approx 1.649$.

For systems with a Maki parameter that is not sufficiently large, the upper critical field must be significantly reduced from the values of h_c , which were estimated in the absence of the orbital pair-breaking effect. However, h_c can be regarded as the index of the strength of the nesting effect for enhancing the stability of the FFLO state. For a fixed strength of orbital pair-breaking effect, the larger the value of h_c , the larger the real upper critical field in the presence of the orbital effect.

In conclusion, the nesting effect for the FFLO state can be significant for perpendicular fields as well as for parallel fields. For the nesting effect in perpendicular fields, the value of t_z must be sufficiently small, and in particular, quasi-low-dimensional systems with open Fermi surfaces favor the present mechanism. The upper limit of t_z decreases as the carrier density decreases.

Acknowledgments The author would like to thank Y. Matsuda for useful discussions on the compound FeSe and related works.

Appendix A: Explicit forms of $f_n(p)$

The integral in Eq. (1) can be carried out explicitly. The results for $n = 0$ are

$$f_0(p) = \begin{cases} -\ln \left| \frac{p}{2} \right| & \text{for } p \geq 1, \\ -\ln \frac{1 + \sqrt{1 - p^2}}{2} & \text{for } p \leq 1, \end{cases}$$

and those for an integer $n \neq 0$ are

$$f_n(p) = \begin{cases} \frac{1}{n} \cos\left(n \arccos \frac{1}{p}\right) & \text{for } p \geq 1, \\ \frac{1}{n} \left(\frac{|p|}{1 + \sqrt{1 - p^2}} \right)^n & \text{for } p \leq 1. \end{cases}$$

The functions $f_2(p)$ and $f_4(p)$ can be expressed as

$$f_2(p) = -\frac{1}{2} + \frac{1}{p^2}, \quad f_4(p) = \frac{1}{4} - \frac{2}{p^2} + \frac{2}{p^4}$$

for $p \geq 1$.

Appendix B: Proof of Eq. (5)

For an arbitrary function $g(x)$ and an arbitrary average $\langle \dots \rangle$ over an arbitrary variable x , it can be proved that if $\langle g \rangle = 1$,

$$\langle g \ln g \rangle \geq 0, \quad (\text{B}\cdot 1)$$

where the equality sign holds for $g(x) = 1$. Applying Eq. (B·1) to the average defined in Eq. (4) and $g = |\gamma_\alpha|^2 / \langle |\gamma_\alpha|^2 \rangle$, we obtain $\sqrt{\langle |\gamma_\alpha|^2 \rangle} \leq \bar{\gamma}_\alpha$, which leads to Eq. (5).

Proof of Eq. (B·1) — It is sufficient to prove this for a simple average such as

$$\langle g \rangle = \frac{1}{n} \sum_{k=1}^n g_k \quad (\text{B}\cdot 2)$$

with an arbitrary positive integer n . In fact, an arbitrary probability function $p(x)$ can be realized by a sufficiently dense distribution of x_k ($k = 1, 2, \dots, n$) on the x -axis as

$$\int dx p(x) g(x) \approx \frac{1}{n} \sum_{k=1}^n g_k,$$

where $g_k = g(x_k)$. For the average defined by Eq. (B·2), the inequality in Eq. (B·1) is easily proved with mathematical induction as follows. For $n = 2$, defining x with $g_1 = 1 + x$ and $g_2 = 1 - x$, $f(x) \equiv \langle g \ln g \rangle$ satisfies $f'(x) \geq 0$ and $f(0) = 0$. Hence, $f(x) \geq 0$. When Eq. (B·1) is satisfied for n , Eq. (B·1) is satisfied for $n + 1$. In fact, assuming $g_{n+1} \leq 1$ without loss of generality,

$$\tilde{g}_k \equiv \frac{ng_k}{n+1-g_{n+1}}$$

satisfies

$$\frac{1}{n} \sum_k \tilde{g}_k \ln \tilde{g}_k \geq 0$$

because of the induction hypothesis. Hence,

$$\frac{1}{n+1} \sum_{k=1}^{n+1} g_k \ln g_k \geq F(g_{n+1}) \geq 0$$

with

$$F(x) \equiv (n+1-x) \ln \frac{n+1-x}{n} + x \ln x.$$

The last inequality holds because $F(1) = 0$ and $F'(x) \leq 0$ for $x \leq 1$. It is evident that the equality sign holds when $g_k = 1$ for all integers k .

Appendix C: Effective Mass Anisotropy

It follows from the definitions

$$\tilde{k}_\mu = \sqrt{\frac{m}{m_\mu}} k_\mu,$$

and $m = \sqrt{m_x m_y}$ that $dk_x dk_y = d\tilde{k}_x d\tilde{k}_y$ and

$$\epsilon_{\mathbf{k}_\parallel}^{\parallel} = \tilde{k}_\parallel^2 / 2m,$$

where \tilde{k}_\parallel and $\tilde{\varphi}$ are defined by

$$(\tilde{k}_x, \tilde{k}_y) = (\tilde{k}_\parallel \cos \tilde{\varphi}, \tilde{k}_\parallel \sin \tilde{\varphi}).$$

We also obtain $\rho = m/2\pi$ and

$$\frac{d^2 \hat{\mathbf{k}}}{S_0} = \frac{d\tilde{\varphi}}{2\pi} \frac{dk_z}{2\pi}.$$

The FFLO vector \mathbf{q} is also transformed as $\tilde{q}_\mu = \sqrt{m/m_\mu} q_\mu$ and

$$\frac{\mathbf{v}_F \cdot \mathbf{q}}{2h_c} = \frac{v_F^{\parallel} \tilde{q}_\parallel}{2h_c} \cos \tilde{\theta} + \frac{t_z q_z}{2h_c} \sin k_z,$$

where $(\tilde{q}_x, \tilde{q}_y) = (\tilde{q}_\parallel \cos \tilde{\theta}_q, \tilde{q}_\parallel \sin \tilde{\theta}_q)$, and $\tilde{\theta} \equiv \tilde{\varphi} - \tilde{\theta}_q$. Hence, all the equations for $m_x \neq m_y$ have exactly the same form as those for $m_x = m_y = m$.

Here, we briefly explain the influence of the above transformation on the orbital pair-breaking effect. The components of the vector potential $\mathbf{A}(\mathbf{r})$, which appears in the gap equation and induces the orbital pair-breaking effect, are scaled with different coefficients that depend on the effective masses, whereas the Zeeman term is unaffected. Hence, the strength of the orbital pair-breaking effect and the Maki parameter depend on the in-plane field direction.⁴⁹⁾

- 1) P. Fulde and R. A. Ferrell, Phys. Rev. **135**, A550 (1964).
- 2) A. I. Larkin and Yu. N. Ovchinnikov, Zh. Eksp. Teor. Fiz. **47**, 1136 (1964); translation: Sov. Phys. JETP, **20**, 762 (1965).
- 3) R. Casalbuoni and G. Nardulli, Rev. Mod. Phys. **76**, 263 (2004).
- 4) Y. Matsuda and H. Shimahara, J. Phys. Soc. Jpn. **76**, 051005 (2007).
- 5) H. Shimahara, in *The Physics of Organic Superconductors and Conductors*, ed. A. G. Lebed (Springer, Berlin, 2008), p. 687.
- 6) J. Wosnitzer, Ann. Phys. (Berlin) **530**, 1700282 (2018).
- 7) J. Singleton, J. A. Symington, M.-S. Nam, A. Ardavan, M. Kurmoo, and P. Day, J. Phys. Condens. Matter **12**, L641 (2000).
- 8) H. A. Radovan, N. A. Fortune, T. P. Murphy, S. T. Hannahs, E. C. Palm, S. W. Tozer, and D. Hall, Nature **425**, 51 (2003).
- 9) A. Bianchi, R. Movshovich, C. Capan, P. G. Pagliuso, and J. L. Sarrao, Phys. Rev. Lett. **91**, 187004 (2003).
- 10) S. Yonezawa, S. Kusaba, Y. Maeno, P. Auban-Senzier, C. Pasquier, K. Bechgaard, and D. Jerome, Phys. Rev. Lett. **100**, 117002 (2008).
- 11) S. Kasahara, Y. Sato, S. Licciardello, M. Čulo, S. Arsenijević, T. Ottenbros, T. Tominaga, J. Böker, I. Eremin, T. Shibauchi, J. Wosnitzer, N. E. Hussey, and Y. Matsuda, Phys. Rev. Lett. **124**, 107001 (2020).
- 12) Here, the term “two-dimensional models” does not mean purely two-dimensional models, but those in which weak three-dimensional interactions that stabilize the long-range order are implicitly taken into account by applying mean-field approximations.
- 13) Below the upper critical field, FFLO states with more than two \mathbf{q} 's can be stable, especially in quasi-low-dimensional systems.⁵⁰⁾ However, because the second-order transition point can be examined by considering a single \mathbf{q} , we do not consider multiple \mathbf{q} states in the present study.
- 14) L. W. Gruenberg and L. Gunther, Phys. Rev. Lett. **16**, 996 (1966).
- 15) H. Shimahara, Phys. Rev. B **80**, 214512 (2009).
- 16) When the orbital pair-breaking effect is sufficiently weak ($\alpha > 1.8$), the vortex and the FFLO oscillation coexist.¹⁴⁾ In the coexistence state,

$\mathbf{q} \parallel \mathbf{H}$ as examined in Ref. 14. However, when the orbital effect is very weak, vortex states with higher Landau-level indices n occur, and the oscillation of the order parameter can have components perpendicular to \mathbf{H} .^{5,15)} The oscillation is reduced to the FFLO oscillation of the pure FFLO state in the limit $n \rightarrow \infty$. Hence, when $\alpha \gg 1$, practically speaking, the FFLO vector has components perpendicular to \mathbf{H} . See also Refs. 26 and 27.

- 17) States with $\Delta(\mathbf{r}) \propto \cos(\mathbf{q} \cdot \mathbf{r})$ have two FFLO vectors, i.e., $\pm \mathbf{q}$, and hence, $\pm \mathbf{q} \parallel \mathbf{H}$; however, for the same reason as that mentioned in Ref. 13, we consider a single \mathbf{q} .
- 18) H. Shimahara and D. Rainer, J. Phys. Soc. Jpn. **66**, 3591 (1997); see also H. Shimahara, J. Supercond., **12**, 469 (1999).
- 19) This effect is called the nesting effect, in analogy with the nesting effect for the SDW and CDW.
- 20) Details of the nesting effect were explained in previous papers, such as Refs. 21, 32, 35, and 42–44.
- 21) H. Shimahara, Phys. Rev. B **50**, 12760 (1994).
- 22) S. Kasahara, T. Watashige, T. Hanaguri, Y. Kohsaka, T. Yamashita, Y. Shimoyama, Y. Mizukami, R. Endo, H. Ikeda, K. Aoyama, T. Terashima, S. Uji, T. Wolf, H. V. Löhneysen, T. Shibauchi, and Y. Matsuda, Proc. Natl. Acad. Sci. U.S.A. **111**, 16309 (2014).
- 23) T. Hanaguri, K. Iwaya, Y. Kohsaka, T. Machida, T. Watashige, S. Kasahara, T. Shibauchi, and Y. Matsuda, Sci. Adv. **4**, eaar6419 (2018).
- 24) T. Shibauchi, T. Hanaguri, and Y. Matsuda, J. Phys. Soc. Jpn. **89**, 102002 (2020).
- 25) K. Kumagai, M. Saitoh, T. Oyaizu, Y. Furukawa, S. Takashima, M. Nohara, H. Takagi, and Y. Matsuda, Phys. Rev. Lett. **97**, 227002 (2006).
- 26) U. Klein, D. Rainer, and H. Shimahara, J. Low. Temp. Phys. (USA), **118**, 91 (2000).
- 27) U. Klein, Phys. Rev. B **69**, 134518 (2004).
- 28) In Sr_2RuO_4 , the FFLO state may occur at high fields parallel to the ab-plane because the antiparallel-spin pairing is considered to be confirmed.⁵¹⁾ The horizontal line node observed in Ref. 52 is compatible with the interlayer pairing.^{29,30)}
- 29) Y. Hasegawa, K. Machida, and M. Ozaki, J. Phys. Soc. Jpn. **69**, 336 (2000).
- 30) H. Shimahara, J. Phys. Soc. Jpn. **89**, 093704 (2020).
- 31) K. W. Song and A. E. Koshelev, Phys. Rev. B **97**, 224520 (2018).
- 32) H. Shimahara, J. Phys. Soc. Jpn. **66**, 541 (1997).
- 33) At $T = 0$, $\Delta_{s0} = \Delta_s$ for the s-wave state with $\gamma_s = 1$, whereas $\Delta_{\alpha 0} = \Delta_\alpha / \gamma_\alpha$ for the other α . For example, see Ref. 35. The dimensionless coupling constant λ_α is expressed as $\lambda_\alpha = g_\alpha N_\alpha(0)$, where $N_\alpha(0) = N(0)[\gamma_\alpha]^2$, and g_α denotes the coupling constant of the pairing interaction for α -wave pairing, which is limited by the cutoff energy ω_c .
- 34) For example, $S_0 = 4\pi$ when $d^2 \hat{\mathbf{k}} = \sin \theta d\theta d\varphi$, and $S_0 = 4\pi^2$ when $d^2 \hat{\mathbf{k}} = d\varphi dk_z$.
- 35) H. Shimahara, J. Phys. Soc. Jpn. **68**, 3069 (1999).
- 36) The internal field is enhanced by a factor $\tilde{\chi}/\chi$, where χ and $\tilde{\chi}$ are the bare susceptibility and the susceptibility renormalized by the repulsive interactions between electrons, respectively. Hence, the FFLO critical field (in terms of the bare external field) is reduced by the factor $\chi/\tilde{\chi} < 1$. On the other hand, because $N_\alpha(0)\Delta_{\alpha 0}^2/2 = \tilde{\chi}H_P^2/2$, H_P is reduced by the factor $\sqrt{\chi/\tilde{\chi}}$. Consequently, H_c/H_P is reduced by the factor $\sqrt{\chi/\tilde{\chi}} < 1$.^{21,53)} Note that the attractive interactions between electrons that induce the superconductivity are effective interactions in which the retardation effect is incorporated. The bare static interactions between electrons on the Fermi surfaces should be repulsive because of the strong Coulomb repulsion, which results in $\tilde{\chi} > \chi$. Hence, if the real H_c is to exceed the real H_P in the presence of the internal-field enhancement, the difference $H_c - H_P (> 0)$ in the absence of the internal-field enhancement must be substantial.
- 37) For a detailed account of the interlayer pairing, see, for example, K. B. Efetov and A. I. Larkin, Zh. Eksp. Teor. Fiz. **68**, 155 (1975) [Sov. Phys. JETP **41**, 76 (1975)]; R. A. Klemm and S. H. Liu, Phys. Rev. B **44**, 7526 (1991); H. Shimahara and M. Kohmoto, Phys. Rev. B **65**, 174502 (2002); H. Shimahara, Phys. Rev. B **72**, 134518 (2005), and the references therein.
- 38) Equation (6) results in $\rho(\xi, \hat{\mathbf{k}}) = m/2\pi$ and $\mathbf{v}_F = (\mathbf{k}_\parallel/m, 2t_z \sin k_z)$, and hence,

$$\frac{\mathbf{v}_F \cdot \mathbf{q}}{2h_c} = \frac{v_F^{\parallel} \tilde{q}_\parallel}{2h_c} \cos \theta + \frac{t_z q_z}{2h_c} \sin k_z,$$

- where $v_F^{\parallel} \equiv |\mathbf{k}_{\parallel}|/m$, and θ denotes the angle between \mathbf{k}_{\parallel} and $\mathbf{q}_{\parallel} = (q_x, q_y)$.
- 39) For example, the expansion of $\epsilon_{\mathbf{k}_{\parallel}}^{\parallel} = -2t(\cos k_x + \cos k_y)$ results in Eq. (7) with $m = 1/t$ for small electron densities.
- 40) If we consider the FFLO state in singlet superconductors, the symmetry in the k_z -direction should be even and odd when the in-plane state is even and odd, respectively. However, the FFLO state can occur in triplet superconductors as long as the pairing occurs between electrons with antiparallel spins.
- 41) The singular behavior at $\mathbf{H} \parallel \mathbf{c}$ is an artifact of the mean-field gap equation applied to the present ideal model with $t_z = 0$, and it must be removed by incorporating the reality, such as the fact that t_z should be finite even when it can be omitted in the gap equation¹²⁾ and $1/q_z$ cannot be smaller than the spacing between the layers.
- 42) H. Shimahara and K. Moriwake, J. Phys. Soc. Jpn. **71**, 1234 (2002); H. Shimahara and S. Hata, Phys. Rev. B **62**, 14541 (2000).
- 43) N. Miyawaki and H. Shimahara, J. Phys. Soc. Jpn. **83**, 024703 (2014).
- 44) K. Itahashi and H. Shimahara, J. Phys. Soc. Jpn. **87**, 083701 (2018); *ibid.* J. Phys. Soc. Jpn. **89**, 024708 (2020).
- 45) See references in Ref. 3–6. For example, see Ref. 18.
- 46) For intralayer pairing, previous studies [for example, H. Adachi and R. Ikeda, Phys. Rev. B **68**, 184510 (2003) and M. Houzet and V. P. Mineev, Phys. Rev. B **4**, 144522 (2006)] have shown that the FFLO state can be stable in perpendicular fields, even in the presence of the orbital pair-breaking effect if the Maki parameter is sufficiently large.
- 47) When the Fermi surfaces are closed and round near the k_z -axis, and we consider a nesting vector \mathbf{q} parallel to \mathbf{c} , they can touch only at a point on the k_z -axis but cannot touch on a curve in most cases. However, the touch at a point yields a lower h_c than that by intersection by curves. Hence, \mathbf{q} becomes longer so that the Fermi surfaces are intersected by a curve. The resulting h_c is lower than the value $h_c = \Delta_{\alpha 0}$ given by the touch on a curve in the system with open Fermi surfaces.
- 48) H. Shishido, R. Settai, D. Aoki, S. Ikeda, H. Nakawaki, N. Nakamura, T. Iizuka, Y. Inada, K. Sugiyama, T. Takeuchi, K. Kindo, T. C. Kobayashi, Y. Haga, H. Harima, Y. Aoki, T. Namiki, H. Sato, and Y. Ōnuki, J. Phys. Soc. Jpn. **71**, 162 (2002).
- 49) For a detailed account of the orbital pair-breaking effect in systems with effective mass anisotropy, see, for example, Y. Suginishi and H. Shimahara, Phys. Rev. B **74**, 024518 (2006); *ibid.* **75** 099902(E) (2007); and H. Shimahara, Phys. Rev. B **80**, 214512 (2009).
- 50) H. Shimahara, J. Phys. Soc. Jpn. **67**, 736 (1998).
- 51) A. Pustogow, Y. Luo, A. Chronister, Y.-S. Su, D.A. Sokolov, F. Jerzenbeck, A.P. Mackenzie, C.W. Hicks, N.Kikugawa, S. Raghu, E.D. Bauer, and S.E. Brown, Nature **574**, 72 (2019).
- 52) S. Kittaka, S. Nakamura, T. Sakakibara, N. Kikugawa, T. Terashima, S. Uji, D.A. Sokolov, A.P. Mackenzie, K. Irie, Y. Tsutsumi, K. Suzuki, and K. Machida, J. Phys. Soc. Jpn. **87**, 093703 (2018).
- 53) S. Takada and T. Izuyama, Prog. Theor. Phys. **41**, 635 (1969).